Biosensors and Bioelectronics 88 (2017) 283–289

Contents lists available at ScienceDirect

Biosensors and Bioelectronics

journal homepage: www.elsevier.com/locate/bios

Biosensor based on a silicon nanowire field-effect transistor functionalized by gold nanoparticles for the highly sensitive determination of prostate specific antigen

Galina Presnova [a], Denis Presnov [b,c], Vladimir Krupenin [c], Vitaly Grigorenko [a], Artem Trifonov [b,c], Irina Andreeva [a], Olga Ignatenko [a], Alexey Egorov [a], Maya Rubtsova [a,*]

[a] Chemistry Faculty, M.V. Lomonosov Moscow State University, Leninskie gori, Moscow, 119991 Russia
[b] Skobeltsyn Institute of Nuclear Physics, M.V. Lomonosov Moscow State University, Leninskie gori, Moscow, 119991 Russia
[c] Faculty of Physics, M.V. Lomonosov Moscow State University, Leninskie gori, Moscow, 119991 Russia

ARTICLE INFO

Article history:
Received 20 May 2016
Received in revised form
6 August 2016
Accepted 17 August 2016
Available online 18 August 2016

Keywords:
Biosensor
Silicon nanowire field-effect transistor
Prostate specific antitigen (PSA)
Gold nanoparticles
Antibodies
Covalent immobilization

ABSTRACT

We have demonstrated label-free and real-time detection of prostate specific antigen (PSA) in human serum using silicon nanowire field effect transistors (NW FETs) with Schottky contacts (Si-Ti). The NW FETs were fabricated from SOI material using high-resolution e-beam lithography, thin film vacuum deposition and reactive-ion etching processes eliminating complicated processes of doping and thermal annealing. This allowed substantial simplifying the transistors manufacturing. A new method for covalent immobilization of half-fragments of antibodies on silicon modified by 3-glycidopropyltrimethoxysilane with thiol groups and 5 nm gold nanoparticles (GNPs) was established. NW FETs functionalized by GNPs revealed extremely high pH sensitivity of 70 mV/pH and enhanced electrical performance in the detection of antigen due to enhanced surface/volume ratio, favorable orientation of antibody active sites and approaching the source of the electric field close to the transistor surface. Si NWFETs were applied for quantitative detection of PSA in a buffer and human serum diluted 1/100. Response time was about 5–10 s, and analysis time per sample was 1 min. The limit of PSA detection was of 23 fg/mL, concentration range of 23 fg/mL–500 ng/mL (7 orders of magnitude). The PSA concentrations determined by the NW FETs in serum were compared with well-established ELISA method. The results matched well with the correlation coefficient of 0.97.

1. Introduction

During the past decades significant improvements in miniaturization of biomedical systems resulted in the establishment of nanoscale bioelectronic devices (Zhang and Lieber, 2016). Among these devices, semiconductor nanowire field-effect transistors (NW FETs) have been attracted a particular attention due to unique electronic properties, ultra small dimensions and label-free detection in real-time mode (Cui and Lieber, 2001; Zhang et al., 2009; Noor and Krull, 2014). The use of silicon for nanosensors has the advantages provided by its features: biocompatibility, unique electronic, optical, and mechanical properties (Peng et al., 2014). The sensitivity of such biosensors is extremely high, it can reach the level from micromoles (Lin et al., 2010) to amol (Maki et al., 2008) and even allows to achieve the detection of single molecules (Hahm and Lieber, 2004; Wang et al., 2005) or particles (Patolsky et al., 2004). NW based biosensors show the advantages in the registration of proteins at extremely low concentrations which is of great importance for early diagnostics of cancer, acute myocardial infarction, and other disorders (Azmi et al., 2014; Zhang et al., 2012; Kong et al., 2012).

Despite the fact that the use of NWs for biosensors is increasingly widespread, only a few of them were applied for the detection of analytes in real biological samples like blood (A. Kim et al., 2009; Stern et al., 2010). High ionic strength of biological fluids reduces the efficiency of conductivity detection on the surface of NWs. Gao et al. (2015) have recently shown that specific modification of silicon NW by a polymer layer of polyethelene glycol increases the effective screening length of the sensor and enables detection of biomolecules in high ionic strength solutions in real-time. In this paper, we report about a new functionalization technique for silicon by small size gold nanoparticles (GNPs) for the improvement of NW FETs electrical performance as peculiar properties of GNPs such as high surface-to-volume ratio, high surface energy, and conductivity were shown to facilitate an electron transfer between biospecific layer and the electrode

* Corresponding author.
E-mail address: mrubtsova@gmail.com (M. Rubtsova).

http://dx.doi.org/10.1016/j.bios.2016.08.054
0956-5663/

surface (Liu et al., 2003). In our method we used 5 nm GNPs for the covalent immobilization of half-fragments of antibodies on gold through their own thiol groups. New functionalization method was compared with chemical modification by different organosilanes. We have utilized NW FETs for the determination of prostate specific antigen (PSA), which is a molecular marker of prostate cancer. NW FET functionalized by GNPs showed the improved sensing performance and the widest detection range for PSA detection. Application of NW FET biosensors on the serum samples showed good correlation with the standard ELISA while significantly simplifying and reducing the analysis time.

2. Materials and methods

2.1. Materials

Inorganic chemicals, 3-aminopropyltrimethoxysilane (APTMS), ethylendiaminetetraacetic acid (EDTA), 3-glycidopropyltriethoxysilane (GOPS), GOPS with thiol groups (GOPS-SH), 1,4-phenylendiizothiocyanate (PDITC), tetrachloroauric (III) acid, 3,3′5,5′-tetramethylbenzidine (TMB), Tween 20, bovine serum albumin (BSA), casein were purchased from Sigma (St. Louis, USA). PSA and two clones of mouse monoclonal antibodies (mAbs) to PSA were provided by JSC "NVO Immunotek" (Moscow, Russia). MAbs and PSA standard solutions were the same which are used in ELISA kit for total PSA determination (JSC "NVO Immunotek"), registered by the Federal Service of Health Care Control of Russian Federation (Registration Certificate FSR 2008/03082, Technical Specifications TY 9398-341-11361534-2004). Specificity of mAbs towards PSA was confirmed by the manufacturer.

2.2. Preparation of GNPs

GNPs with an average diameter of 25 nm were obtained by the reduction of tetrachloroauric (III) acid with sodium citrate as described by Frens (1973). GNPs with an average diameter of 5 nm were prepared by the reduction of tetrachloroauric (III) acid with sodium borohydride in the presence of EDTA (Bogatyrev et al., 1994): 0.2 mL of a freshly prepared 1% tetrachloroauric (III) acid and 0.5 mL 0.2 M potassium carbonate were added to 45 mL of 0.3 mM EDTA at 4 °C with stirring. Then, 0.125 mL of 0.5% sodium borohydride was added, and a red-brown sol with an absorption peak of 510 nm was formed.

2.3. Fragmentation of mAbs into symmetric half-fragments

MAbs against PSA in 0.1 M phosphate buffer pH 6.0 containing 0.15 M NaCl and 5 mM EDTA were fragmented into two symmetric half-fragments using 12 mg/mL 2-MEA for 1.5 h at 37 °C and then desalted on a 15-mL Sephadex G-25 column equilibrated with 50 mM Tris pH 8.5 containing 0.15 M NaCl and 5 mM EDTA.

2.4. Conjugation of mAbs half-fragments with GNPs

A solution of second clone mAbs half-fragments (100 μM) was mixed with 1 mL suspension of 25 nm GNPs (pH 7.0 adjusted by freshly prepared Na_2CO_3) and incubated for 2 h at room temperature. Then the suspension was centrifuged at 11,000 rpm for 30 min using a 5810R centrifuge (Eppendorf, Germany). The supernatant was discarded and the pellet was dissolved in 0.01 M K-phosphate buffer with 0.15 M NaCl, pH 7.4 (PBS).

2.5. Functionalization of silicon wafers

The surface of the silicon wafers was purified with oxygen plasma (30 Pa, 25 Wt) for 30 min using a RDE-300 reactive ion-etching instrument (Alcatel, France) and then it was chemically modified by following methods:

2.5.1. Modification with APTMS and PDITC

silicon wafers were heated for 1 h at 100 °C and placed in a vessel containing a 10% APTMS in ethanol. After overnight incubation, the samples were washed three times with ethanol and then with distilled water. The dried samples were incubated in an oven at 100 °C for 10 min and then placed in a solution of 6 mg PDITC in dimethylformamide containing 10% pyridine and stirred for 1 h at room temperature. The resulting samples were washed three times with methanol and deionized water at stirring.

2.5.2. Modification with GOPS

silicon wafers were incubated in 0.2 M solution of GOPS in toluene overnight at 70 °C, then they were washed twice with toluene, methanol, and water at stirring and air dried.

2.5.3. Modification with GOPS-SH and small GNPs

silicon wafers were functionalized by GOPS-SH similarly to the method described above for the GOPS. Then a suspension of 5 nm GNPs was added, incubated overnight at 4 °C, washed twice with PBS.

2.5.4. Immobilization of mAbs

1 μL of mAbs (or their fragments) in PBS (100 μg/mL) was dropped on the modified surface of silicon wafers and incubated for 1 h at 37 °C. Then the samples were washed three times with PBS containing 0.1% Tween 20 (PBST). The surface was blocked with 1% BSA and 1% casein in PBS for 1 h at 37° C.

2.6. Characterization of modified silicon by atomic force microscopy (AFM) and sandwich immunoassay

The samples of silicon were measured using scanning probe microscope AIST-NT SPM (SmartSPM-1000) at ambient conditions. Surface scratching was made in a contact mode of AFM at constant force regime (load 45 nN, velocity 1 μm/s). Topography profiles were obtained in a tapping mode with Pt coated conductive cantilevers (Microscience, model N14/Pt) with a spring constant ranged from 6 to 10 N/m and the cantilever tips (20 nm radius).

To compare the silicon modification methods, the formation of sandwich antigen-antibody complexes was studied. Incubation of mAbs with PSA and then with a conjugate of second clone mAbs with GNPs or peroxidase was performed in PBST for 1 h at 37 °C. Antibodies nonspecific to PSA were used as control. GNPs on the silicon surface were detected by a Supra 40 field emission scanning electron microscope (Carl Zeiss, Germany) with an InLens secondary electron detector integrated in the microscope column. Activity of peroxidase was detected optically with TMB and H_2O_2 as substrates.

2.7. Fabrication of NW FETs

SOI wafers (UNIBOND® wafers, Soitec) with upper silicon layer of 110 nm and buried oxide layer of 200 nm were used for fabrication of NWs, which is described in the Supplementary materials (Fig. S1). Final structure of sensing element with contact pads covered by dielectric is shown in Fig. S2. The NW channel had a length of 3 μm and a width of about 100 nm. Then it was mounted into ceramic chip-carrier and the contacts were connected by 25 μm Al wire using ultrasonic wire bonder (WestBond, USA). Additional insulation of the contacts and connecting wires was performed by silicone sealant. Finally the sensor has the form of a small cap with the open window (about 500 μm in diameter) at

the bottom allowing central working area with the transistors to be reachable for the analyte. The biosensors were stored at 4 °C for two months with no apparent loss of activity.

2.8. Electrical measurements, determination of PSA in a buffer and human serum

Measurements were carried out in the microfluidic system, consisted of the measuring cell, the low-noise current pre-amplifier, interface electronics unit, and a personal computer. They were performed in static mode without fluid flow, which ensures stable and reproducible response. The response signals were measured in real time simultaneously by two transistor-sensors, spaced about 50 μm from each other. 100 μL of the solution was dropped on the chip surface covered with an insulating silicone sealant. The conductivity of NW was modulated by the voltage at the main gate – silicon substrate of SOI wafer. Measurements were performed at positive voltages on the main (substrate) gate, which corresponds to the inverse (electronic) conductivity channel of the transistor. AgCl reference electrode served as an additional gate for the transistor was immersed in the solution drop for adjusting its operating point.

Initial measurements of the NW FETs electrical characteristics were done by immersing the NWs in 0.01 × PBS buffer solution using an open chamber at room temperature. The registration of NW FET response to pH changes was performed as described by Bergveld (2003). 100 μL of the buffer with different pH values were dropped on NW. The dependencies of transport current I versus main gate voltage U_{SG} were measured at fixed voltage (U_{SD}=50 – 200 mV) between the drain and source and on the reference electrode (U_E=300 mV). The operating point of the transistors was chosen in subthreshold region (U_{SG}=6 V). In subsequent measurements the operating point was adjusted by a voltage on reference electrode. The current preamplifier had the conversion factor of $10^8 - 10^9$ V/A and the level of current noise was less than 50 fA/$\sqrt{}$Hz at frequencies above 10 Hz.

Electrical detection of PSA interaction with mAbs immobilized of the NWs was performed in 0.01 × PBS pH 8.0. First, a baseline was obtained from the flowing buffer solution. After it was stabilized, various concentrations of PSA in the same buffer were applied, and the change in the current was registered. BSA in a concentration of 1 μg/mL was used for control experiments. Limit of PSA detection (LOD) was calculated as mean conductivity for PSA free solution (0 ng/mL PSA) plus 3 SD (n=10).

To measure PSA in human blood serum, the samples were diluted 1/100 in 0.01 x PBS pH 8.0 and then applied to the NWs as described above. ELISA kit for quantitative determination of total PSA concentration was used accordingly to manufacturer instructions.

3. Results and discussion

3.1. Functionalization of silicon by covalently immobilized mAbs

The small size of nanodevices imposes certain requirements on the density and uniformity of the biorecognition layer. In order to achieve optimal density and uniform distribution of chemical groups for the covalent attachment of mAbs we compared different approaches for silane functionalization of silicon by: (a) aminopropyltrimetoxysilane (APTMS) in a combination with bifunctional reagent 1,4-phenylene diisothiocyanate (PDITC), (b) 3-glycidopropyltriethoxysilane (GOPS), (c) GOPS-SH followed by covalent attachment of small size GNPs through the interaction of thiol groups with gold. 5 nm GNPs were obtained by the reduction of tetrachloroauric (III) acid with sodium borohydride in the presence of EDTA. Fig. 1 presents the schemes for silicon functionalization. Specific mAbs of first clone were covalently attached to the pretreated silicon via amino-groups (a, b), and thiol groups of half-fragments (c). To liberate the thiol groups, intact antibody molecule was split into two symmetric half-fragments by the reduction with 2-MEA. One half-fragment contains one heavy chain and one light chain, and its antigen binding site is not destroyed. As we have shown earlier (Karyakin et al., 2000), immobilization of half-fragments on gold via their thiol groups maintains high antigen binding constants and provides favorable orientation in terms of the similar distance between the binding site of the antibody and the surface of the gold support, which does not cause the distribution of the apparent affinity constants.

To estimate the binding density of mAbs immobilized we studied the formation of sandwich immune complexes composed of an antigen molecule and two molecules of antibodies, one immobilized on the modified silicon and the second labeled with 25 nm GNPs or peroxidase. Scanning electron microscopy (SEM) was used for the visualization of GNPs-labels on the surface. Fig. S3 shows a fragment of silicon surface involving a boundary between a spot with specific mAbs and a control area without antibodies immobilized. GNPs are clearly visible in the test area, and their distribution is uniform. The difference in the number of GNPs observed in the test and control zones is absolutely clear. Thus, each nanoparticle of 25 nm on the surface is a part of an immune complex, and total GNPs number is proportional to the total number of the complexes formed on the surface. Fig. S4 shows the distribution of GNPs-labels on silicon surface functionalized by different techniques. The maximal density of GNPs was detected for silicon modified with APTMS/PDITC (430 ± 38 GNPs/μm^2) and silicon modified by GOPS-SH/small GNPs (360 ± 45 GNPs/μm^2), while amount of GNPs detected on silicon modified with GOPS was 3 times less (120 ± 15 GNPs/μm^2). So far as not all immune complexes may be revealed by a conjugate of second clone mAbs with GNPs of 25 nm due to steric hindrance, we also detected them with a conjugate of second clone mAbs with peroxidase followed by optical detection of the enzyme (Fig. S5). Comparable binding activity of the mAbs was observed on silicon modified by APTMS/PDITS and GOPS-SH/small GNPs, while the activity on the silicon modified by GOPS was lower. It means that GOPS processing gives fewer chemical groups for antibody immobilization compared with APTMS pretreatment. Despite this fact, both functionalization techniques with APTMS/PDITS and GOPS-SH/small GNPs provide similar antigen binding efficacy, which may be explained by a favorable mAbs orientation when they are immobilized via thiol groups located far to the active sites.

3.2. Fabrication of the NW FETs and electrical performance

NW FETs were fabricated by the technology previously established (Presnov et al., 2013). The body of the transistor with NW channel and the low-scale electrodes were formed by e-beam lithography, evaporation of Al mask and anisotropic reactive ion etching of top Si layer in fluorine plasma through the mask. Ti electrodes formed contacts to low-scale Si electrodes of the transistor body. Since the silicon substrate played the role of a gate electrode for the transistors, and the original oxide layer had a number of defects in the large-scale area, the additional isolation 200 nm SiO_2 layer was deposited on the chip except the area with the transistor structures before deposition of Ti electrodes. Our biosensors were based on silicon NW FETs with Schottky contacts (Si-Ti) (Koo et al., 2005). Schottky barrier FETs have some important advantages in a comparison with traditional doped source and drain structures: simple and low temperature fabricating process, lower leakage current and parasitic resistance at sub-100 nm range, elimination of doping or silicide formation and

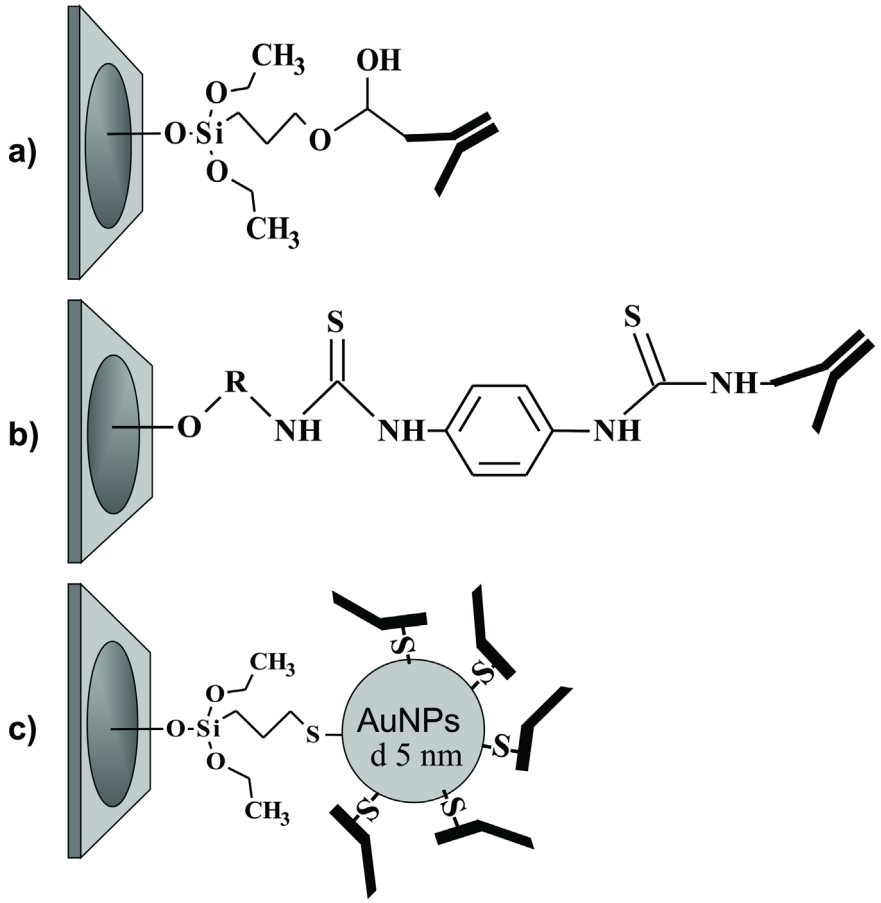

Fig. 1. Schematic illustration of silicon functionalization methods studied in the work.

subsequent thermal annealing processes. The presence of Schottky contacts do not affect the biosensor sensitivity as equivalent resistance at the Ti-Si contacts has the value of about 1 kOhms (Presnov et al., 2013), which is several orders less than NW resistance. After fabrication the NWs were functionalized by GOPS-SH/5 nm GNPs or APTMS/PDITS followed by the covalent attachment of mAbs. Fig. 2 (A–D) shows SEM images of corresponding NW FETs.

The response of the biosensors to external stimuli was registered at the subthreshold region characterized by low bias voltage and transport current through the transistors (Park et al., 2007). As we showed earlier, the mode of low currents is preferable for NW FETs both in terms of low self noises (current shot noise) and low heating of the NWs (Presnov et al., 2013). It is explained by decreasing of the charge concentration near the NW surface which increases the screening length of the NW. Electric field of charges located near the NW surface penetrates the entire thickness of the NW and their influence on the NW conductivity is closed to maximum. It results in higher sensitivity of NWs to external charges near their surface in this regime.

The conductivity of the NW channel depends on local variation of the field or concentration of hydrogen ions (pH) connecting with the surface of modified silicon. Accordingly van Hal et al. (1995), the pH sensitivity of the NW FET can be estimated as:

$$\delta\Psi_0/\delta\mathrm{pH} = \Delta U_E/\Delta\mathrm{pH}$$

where $\delta\Psi_0$ – is change of the insulator–electrolyte potential, U_E – is voltage on reference electrode.

We measured the dependence of current on time in the buffer with two different pH values (pH=7.0 and pH=5.0). The measurements were made by applying fixed source–drain and source–gate voltages, and then the voltage on reference electrode was changed to adjust the signal at pH=5.0 to its initial level at pH=7.0 (Fig. 2E, F). One can see that the current level for the transistor modified by GOPS-SH/ 5 nm GNPs in a buffer with pH 7.0 and U_E 500 mV coincides with the current for a buffer with pH 5.0 and U_E 360 mV, and the current level for the transistor modified by APTMS/PTIDC in a buffer with pH 7 and U_E 350 mV coincides with the current for a buffer with pH 5 and U_E 225 mV. Accordingly, the pH sensitivity is 70 ± 3 mV/pH and 62 ± 3 mV/pH for NWs modified by GOPS-SH/5 nm GNPs and APTMS/PTIDC, respectively. The extremely high sensitivity provided by the sensor functionalized with small GNPs can be explained by significant improvement of NWs surface-to-volume ratio by GNPs which leads to increase of local concentration of hydrogen ions near the surface of modified silicon.

3.3. Detection of PSA on the NWFET

The principle of analyte detection by the NW FETs consists in registration of changes in the transport current caused by variations of transistor surface charge at PSA interaction with the immobilized antibodies. Several papers were published recently dealing with theoretical calculations and experimental studies evaluating the sensitivity of the NWs, depending on their configuration and the Debye screening length (De Vico et al., 2011; Li et al., 2011). The Debye length (λ_D) presents the thickness of an electrical double layer near the gate dielectric/buffer interface in an electrolyte buffer. It corresponds to the average distance, at which the electric field penetrates into the buffer. The Debye-Hückel law is carried out in the buffers with a low ionic strength, and the Debye length can be calculated by the formula:

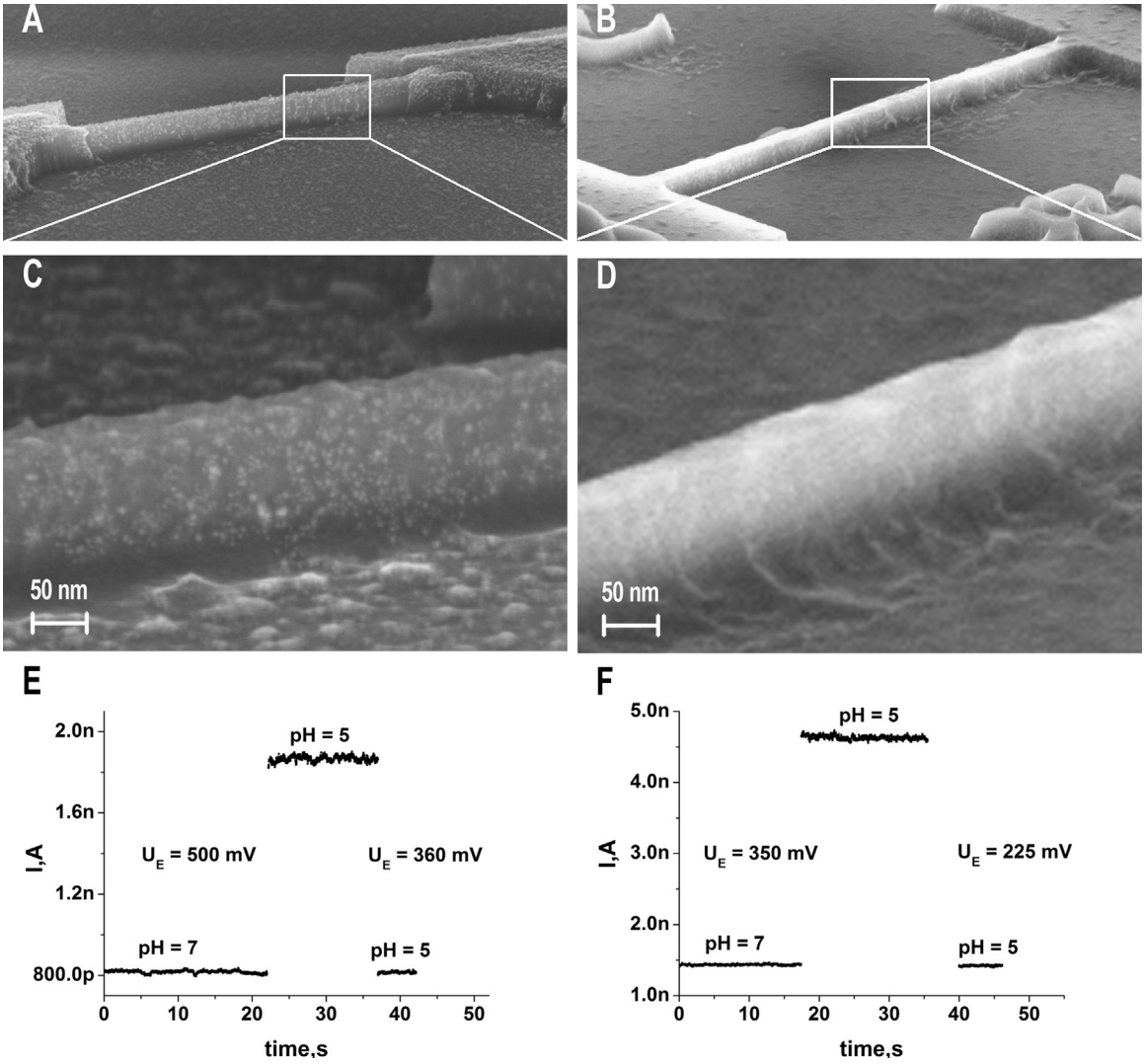

Fig. 2. A, C – SEM images of NW FETs, functionalized by GOPS-SH/ 5 nm GNPs; B, D – SEM images of NW FETs, functionalized by APTMS/PTIDC; E – response to the change of buffer pH for NW FETs functionalized by GOPS-SH/ 5 nm GNPs; F – response to the change of buffer pH for NW FETs functionalized by APTMS/PTIDC.

$$\lambda_D = \sqrt{\varepsilon\varepsilon_0 \kappa T / 2Ie_0^2} \quad (1)$$

where e_0 is electron charge, ε is halfdielectric permittivity of the solvent, ε_0 is dielectric permittivity of the vacuum; k is the Boltzmann constant, T is absolute temperature, I is ionic strength of the solution.

The ionic strength can be calculated as follows:

$$I = \frac{1}{2} \sum n_{i0} z_i^2 \quad (2)$$

where n_{i0} – is molar concentration of the ions (mol/L), z_i – is ion charge.

Eq. (1) shows that the Debye length depends strongly on the ionic strength of the aqueous solution (Stern et al., 2007). It decreases in the solutions with high ionic strength like human serum (analog 1 × PBS), where λ_D is about 0.7 nm. This parameter is significantly lower compared to the thickness of antibodies immobilized on the modified silicon, which was estimated to be appr. 2 nm (Awsiuk et al., 2013). Therefore, in order to increase the sensitivity of the sensor, it is necessary to reduce the ionic strength of buffer.

To measure the thickness of GOPS-SH layer on our NWs, we scratched a small fragment (250 × 250 nm) of silicon surface by AFM cantilever with an increased strength of 45 nH to remove the modifying layer (Fig. S6). The thickness was estimated to be not greater than 1.5–2 nm (insert on Fig. S7). J. Kim et al. (2009) estimated earlier the thickness of APTES layer as ranging from 0.8 to 1.3 nm. The thickness of antibodies and their half-fragments do not exceed 2 nm (Awsiuk et al., 2013). We calculated the Debye lengths for various concentration of buffer ions accordingly to Eq. (1). The Debye length for 0.01 × PBS was about 7 nm, which exceeds sufficiently the thickness of estimated above antibodies layer. Further measurements were carried out in this buffer.

Determination of PSA on the NW FETs was based on a direct binding of the antigen with antibodies or their fragments, which resulted in apparent current change in response to variations of electric field near the surface in a result of antigen binding. Fig. 3 presents the plots of the normalized current change when PSA in 0.01 × PBS was dropped on the NW FETs functionalized by two techniques. The higher signals were determined for NWs modified by GOPS-SH/small GNPs. We suppose the increase in transistor response is related to amplification of electrical field near the NW surface in the presence of GNPs. The electrical field is inversely proportional to the square of the distance from charge to the surface. When NWs are modified with chemical reagents like APTMS there is at least 3–4 nm distance between immune complexes and the NW surface. When antibodies half-fragments are immobilized directly on the GNPs via thiol groups, their active

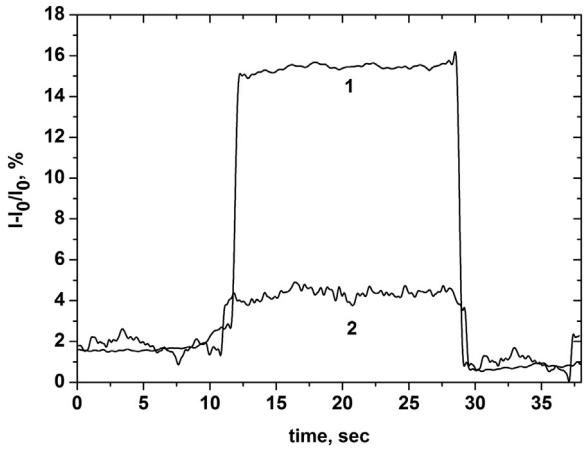

Fig. 3. Plots of normalized current change versus time for NW FETs modified with GOPS-SH/5 nm GNPs (1) and APTMS/PDITC (2).

sites are oriented towards the nanoparticles. It approaches the source of electrical field directly to the surface, and conductive gold nanoparticles may promote an overflow of charge on the nanowire.

Fig. S7 shows the dependence of the current change on pH of the buffer. Signal inversion was detected at pH range of 6.8–7.5, which matches the isoelectric point of PSA of 7.5 accordingly to Huber et al. (1995). At pH higher 7.5 the signal value increased slightly, while at low pH values there was a significant decrease in the response of the transistor. To improve the assay reproducibility, further measurements were made at pH 8.0.

Calibration curve for the detection of PSA in 0.01 × PBS buffer with NW FETs functionalized by GNPs is shown in Fig. 4A. The maximum response to antigen solutions was reached in about 5–10 s, the signal was stable for at least several minutes. Analysis time per sample including signal detection and washing was 1 min. Control experiment with 1 μg/mL of BSA showed no change in the conductance of the NW FETs above the noise level. The rapid changes in the conductivity of the NWs indicate that we registered the binding of antigen molecules which are located close to the NW surface. NW FETs retained about 89% of activity after 80 injections.

The method exhibited a dynamic range for PSA detection in a buffer from 23 fg/mL to 500 ng/mL (7 orders of magnitude) and a detection limit of 23 fg/mL (0.7 fM). Table 1 presents the data on PSA detection by various biosensors proposed in recent years. Our biosensor is highly sensitive comparing with the biosensors based on electrodes and reveals lower sensitivity only in a comparison with NW FETs biosensors described by Gao et al. (2014) and Lu et al. (2015). This could be due to the differences in the NWs size, Abs properties and measurement modes. Functionalization of silicon with spherical NPs increases the surface to volume ratio and improves favorable orientation of Abs active sites to the surface as well. This increases the number of individual acts of the antigen-antibody interaction which occurs in the recorded area on the NW and explains the widest PSA concentration range comparing with other methods.

3.4. Using the NWFETs for the determination of total PSA in human serum

The NW FETs were then examined for real-time quantitative detection of PSA in human serum. PSA standard samples were prepared in PBS containing 10% fetal bovine serum (FBS). PSA standard samples and 13 serum samples were diluted 1/100 with 0.01 × PBS pH 8.0 and then measured by NW FET biosensors. Fig. 4B presents calibration curve for PSA in serum. Concentration range corresponds to the requirements of clinical diagnosis for total PSA quantitative determination (Wu et al., 2007). Sensitivity of PSA detection in serum determined from the curve slope is even higher than that in the buffer. The results obtained for measuring 13 serum samples are listed in Table 2. The NW FETs measured both normal and increased PSA concentrations successfully, which matches the request of clinical standards. PSA concentrations determined by NW FETs were compared with standard ELISA method. A very good correlation was achieved between two methods with a coefficient of 0.97.

4. Conclusions

We developed a label-free and fast assay based on the NW FETs for determination of PSA in human serum. NWs functionalization was performed by a new method using GOPS-SH and 5 nm GNPs, which provides covalent oriented attachment of antibody half-fragments via their thiol groups. The use of the GNPs results in improved electrical performance of the transistor and its higher sensitivity to pH. NW FETs demonstrated low limit of analyte detection together with the widest dynamic concentration range. The presented biosensor was applied for PSA detection in human serum, yielding promising results for real samples assessment. The sensitivity achieved by the NW FETs was 2 orders of magnitude

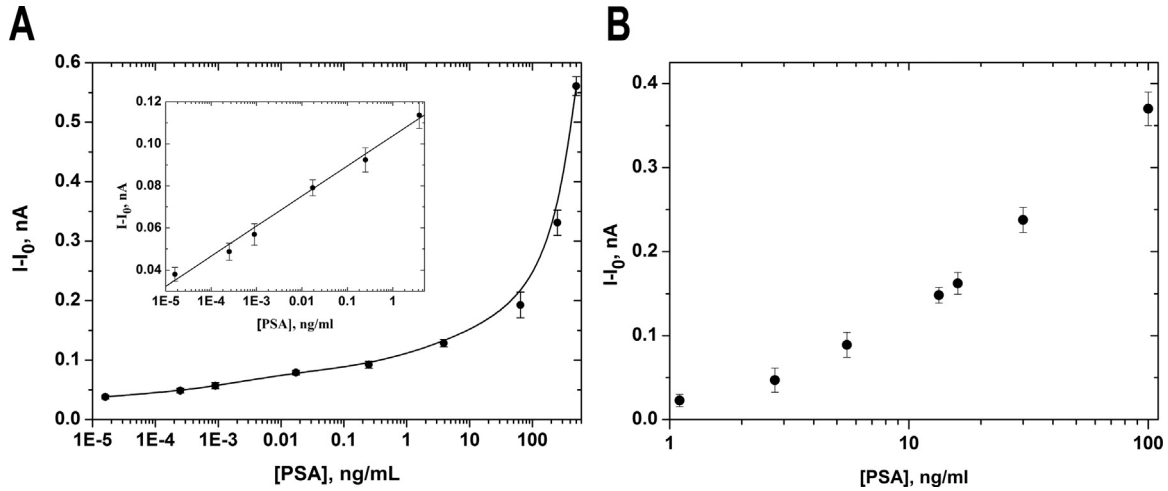

Fig. 4. Calibration curve for the detection of PSA in 0.01 × PBS pH 8.0 (A) and PSA standards in fetal bovine serum diluted 1/100 in 0.01 × PBS pH 8.0 (B).

Table 1
Analytical performances of different biosensors developed recently for quantitative determination of PSA.

Biosensor type//surface modificator	Limit of PSA detection, ng/mL	Detection range, ng/mL	Assay time	Reference
Si NW FETs//GORS-SH and small GNPs	2.3×10^{-5}	$2.3 \times 10^{-5} - 500$	1 min	In this study
Si NW FETs/combination of both n- and p-type nanowires// APTES and glutaraldehyde	1.0×10^{-6}	1.0×10^{-6}–10^{-1}	Several minutes	(Gao et al., 2014)
Microfluidic integrated Si FET arrays//APTES and glutaraldehyde	1.0×10^{-6}	1.0×10^{-6}–1	From 1 to several minutes	(Lu et al., 2015)
Microcontact-PSA imprinted capacitive biosensor chip on gold electrodes	8.0×10^{-5}	$8.0 \times 10^{-5} - 1$	3 min and 20 min for equilibration and regeneration	(Ertürk et al., 2015)
Biosensor based on nanowell arrays with gold base electrodes, EIS detection	1.0×10^{-4}	1.0×10^{-3}–1000	3 min	(Selvam et al., 2015)
Potentiometric competitive immunoassay using Nafion-modified gold electrode, nanospheres, and charged GNPs with immobilized antibodies	4.0×10^{-2}	0.1 – 50	Incubation for 30 min and time for potentiometric detection	(Zhang et al., 2014)

Table 2
Determination of PSA in human serum.

Sample number	PSA detected by NW FET, ng/mL	PSA detected by ELISA, ng/mL
1	0,9 ± 0,5	0,4 ± 0,02
2	1,3 ± 0,7	1,2 ± 0,05
3	2,7 ± 0,7	1,8 ± 0,1
4	4,5 ± 1,3	2,8 ± 0,2
5	4,6 ± 1,6	3,6 ± 0,1
6	4,6 ± 1,8	4,1 ± 0.1
7	5,3 ± 0,8	4,5 ± 0,2
8	5,9 ± 1,4	5,5 ± 0,2
9	12,1 ± 1,0	13,7 ± 0,5
10	13,3 ± 0,7	14,2 ± 0,5
11	15,1 ± 2,1	16,0 ± 0,3
12	22,8 ± 2,4	19,3 ± 0,7
13	31,1 ± 1,5	30,0 ± 0,8

higher than the well-established ELISA method. Future work should focus on optimization of NW length and diameter in order to improve LOD and the development of multichip based on several NWs with different specific antibodies, as the detection range of more than 7 orders of magnitude is very promising in terms of the simultaneous determination of different compounds in one assay.

Acknowledgments

We thank Ivan Bozhiev for assistance in sample fabrication. The work was supported by the Russian Foundation for Basic Research (RFBR), Russia (Grants 13-04-01137 and 16-29-03266).

Appendix A. Supplementary material

Supplementary data associated with this article can be found in the online version at http://dx.doi.org/10.1016/j.bios.2016.08.054.

References

Awsiuk, K., Budkowski, A., Psarouli, A., Petrou, P., Bernasik, A., Kakabakos, S., Rysz, J., Raptis, I., 2013. Colloids Surf. B: Biointerfaces 110, 217–224.
Azmi, M.A.M., Tehrani, Z., Lewis, R.P., Walker, K.-A.D., Jones, D.R., Daniels, D.R., Doak, S.H., Guy, O.J., 2014. Biosens. Bioelectron. 52, 216–224.
Bergveld, P., 2003. Sens. Actuators B 88, 1–20.
Bogatyrev, V.A., Dykman, L.A., Schegolev, S.Yu., 1994. Patent 2013374 Russian Federation.
Cui, Y., Lieber, C.M., 2001. Science 291, 851–853.
De Vico, L., Sorensen, M.H., Iversen, L., Rogers, D.M., Sorensen, B.S., Brandbyge, M., Nygard, J., Martinez, L., Jensen, J.H., 2011. Nanoscale 3, 706–717.
Ertürk, G., Hedstrom, M., Tümer, M.A., Denizli, A., Mattiasson, B., 2015. Anal. Chim. Acta 891, 120–129.
Frens, G., 1973. Nat. Phys. Sci. 241, 20–22.
Gao, N., Zhou, W., Jiang, X., Hong, G., Fu, T.-M., Lieber, C.M., 2015. Nano Lett. 15, 2143–2148.
Gao, A., Lu, N., Dai, P., Fan, C., Wang, Y., Li, T., 2014. Nanoscale 6, 13036–13042.
Hahm, J., Lieber, C.M., 2004. Nano Lett. 4, 51–54.
Huber, P.R., Schmid, H.P., Mattarelli, G., Strittmatter, B., van Steenbrugge, G.J., Maurer, A., 1995. Prostate 27, 212–219.
Karyakin, A.A., PresNova, G.V., Rubtsova, M. Yu, Egorov, A.M., 2000. Anal. Chem. 72, 3805–3811.
Kim, A., Ah, C.S., Park, C.W., Yang, J.-H., Kim, T., Ahn, C.-G., Park, S.H., Sung, G.Y., 2009. Biosens. Bioelectron. 25, 1767–1773.
Kim, J., Seidler, P., Wan, L.S., Fill, C., 2009. Colloid Interface Sci. 329, 114–119.
Kong, T., Su, R., Zhang, B., Zhang, Q., Cheng, G., 2012. Biosens. Bioelectron. 34, 267–272.
Koo, S.M., Edelstein, M.D., Li, Q., Richter, C.A., Vogel, E.M., 2005. Nanotechnology 16, 1482–1485.
Lin, T.-W., Hsieh, P.-J., Lin, C.-L., Fang, Y.-Y., Yang, J.-X., Tsai, C.-C., Chiang, P.-L., Pan, C.-Y., Chen, Y.-T., 2010. PNAS 107, 1047–1052.
Li, J., Zhang, Y., To, S., You, L., Sun, Yu, 2011. ACS Nano 5, 6661–6668.
Liu, S., Leech, D., Ju, H., 2003. Anal. Lett. 36, 1–19.
Lu, N., Gao, A., Dai, P., Mao, H., Zuo, X., Fan, C., Wang, Y., Li, T., 2015. Anal. Chem. 87, 11203–11208.
Maki, Y.-T., Mishra, N.N., Cameron, E.G., Filanoski, B., Rastogi, S.K., Maki, G.K., 2008. Biosens. Bioelectron. 23, 780–787.
Noor, M.O., Krull, U.J., 2014. Anal. Chim. Acta 825, 1–25.
Park, I., Li, Z., Pisano, A.P., Williams, R.S., 2007. Nano Lett. 7, 3106–3111.
Patolsky, F., Zheng, G., Hayden, O., Lakadamyali, M., Zhuang, X., Lieber, C.M., 2004. PNAS 101, 14017–14022.
Peng, F., Su, Y., Zhong, Y., Fan, C., Lee, S.T., He, Y., 2014. Acc. Chem Res 47, 612–623.
Presnov, D.E., Amitonov, S.V., Krutitskii, P.A., Kolybasova, V.V., Devyatov, I.A., Krupenin, V.A., Soloviev, I.I., 2013. Beilstein J. Nanotechnol. 4, 330–335.
Selvam, A.P., Prasad, S., Barrett, T.W., Kazmierczak, S.C., 2015. Nanomedicine 10, 2527–2536.
Stern, E., Vacic, A., Rajan, N.K., Criscione, J.M., Park, J., Ilic, B.R., Mooney, D.J., Reed, M. A., Fahmy, T.M., 2010. Nat. Nanotechnol. 5, 138–142.
Stern, E., Wagner, R., Sigworth, R.J., Breaker, R., Fahmy, T.M., Reed, M.A., 2007. Nano Lett. 7, 3405–3409.
van Hal, R.E.G., Eijkel, J.C.T., Bergveld, P., 1995. Sens. Actuators B 24, 201–205.
Wang, W.U., Chen, C., Lin, K., Fang, Y., Lieber, C.M., 2005. PNAS 102, 3208–3212.
Wu, J., Fu, Z., Yan, F., Ju, H., 2007. Trends. Chem 26, 679–689.
Zhang, A., Lieber, C.M., 2016. Nano-Bioelectron. Chem. Rev. 116, 215–257.
Zhang, B., Liu, B., Chen, G., Tang, D., 2014. Biosens. Bioelectron. 53, 465–471.
Zhang, G.-J., Chai, K.T., Luo, H.Z., Huang, J.M., Tay, I.G., Lim, A.E., Je, M., 2012. Biosens. Bioelectron. 35, 218–223.
Zhang, G.-J., Chua, J.H., Chee, R.E., Agarval, A., Wong, S.M., 2009. Biosens. Bioelectron. 24, 2504–2508.